12.2 Rotational motion of deformed shapes

12.2.1 The Bohr Hamiltonian

In contrast to the discussion of section 12.1; other small amplitude harmonic vibrations can occur around a non-spherical equilibrium shape. So, the potential $U(\alpha_{2\mu})$ (see equation (12.4)) in the collective Hamiltonian can eventually show a minimum at a non-zero set of values $(\alpha_{2\mu})_0$. In this case, a stable deformed shape can result and thus, collective rotations described by the collective variables $\alpha_{2\mu}$, in the laboratory frame. For axially symmetric objects, rotation around an axis, perpendicular to the symmetry axis (see figure 12.11) can indeed occur. Such modes of motion are called collective rotations. We shall also concentrate on the quadrupole degree of freedom since it is this particular multipolarity ($\lambda = 2$) which plays a major role in describing low-lying, nuclear collective excitations.

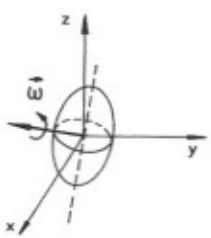

Figure 12.11. Rotational motion of a deformed nucleus (characterized by the rotational vector $\vec{\omega}$). The internal degrees of freedom are described by β and γ (see equation (12.30) and the external, rotational degrees of freedom are denoted by the Euler angles Ω (taken from Iachello 1985).

Starting from a stable, deformed nucleus and a set of intrinsic axes, connected to the rotating motion of the nucleus as depicted in the lab frame, one can, in general, relate the transformed collective variables $a_{\lambda\mu}$ to the laboratory $\alpha_{\lambda\mu}$ values. The transformation is described, according to (appendix B):

$$\begin{aligned} Y_{\lambda\mu}(\text{rotated}) &= \sum_{\mu'} D^{\lambda}_{\mu'\mu}(\Omega) Y_{\lambda\mu'}(\text{lab}) \\ a_{\lambda\mu} &= \sum_{\mu'} D^{\lambda}_{\mu'\mu}(\Omega) \alpha_{\lambda\mu'}. \end{aligned} \tag{12.29}$$

Thereby, the nuclear radius $R(\theta, \varphi)$ remains invariant under a rotation of the coordinate system.

For axially symmetric deformations with the z-axis as symmetry axis, all $\alpha_{\lambda\mu}$ vanish except for $\mu = 0$. These variables $\alpha_{\lambda 0}$ are usually called β_λ. For a quadrupole deformation, we have five variables $\alpha_{2,\mu}$ ($\mu = -2, \ldots + 2$). Three of them determine the orientation of the liquid drop in the lab frame (corresponding to the Euler angles Ω). Using the transformation from the lab into the rotated, body-fixed axis system, the five $\alpha_{2\mu}$ reduce to *two* real independent variables a_{20} and $a_{22} = a_{2-2}$ (with $a_{21} = a_{2-1} = 0$). One can define the more standard parameters

$$\begin{aligned} a_{20} &= \beta \cos\gamma \\ a_{22} &= \frac{1}{\sqrt{2}}\beta \sin\gamma. \end{aligned} \tag{12.30}$$

Using the Y_{20} and $Y_{2\pm 2}$ spherical harmonics in the intrinsic system, we can rewrite $R(\theta, \varphi)$ as

$$R(\theta,\varphi) = R_0 \left\{ 1 + \beta \sqrt{\frac{5}{16\pi}} (\cos\gamma (3\cos^2\theta - 1) + \sqrt{3}\sin\gamma \sin^2\theta \cos^2\varphi) \right\}. \tag{12.31}$$

In figure 12.12, we present these nuclear shapes for $\lambda = 2$ using the polar angles.

(a) γ values of 0°, 120° and 240° yield prolate spheroids with the 3, 1 and 2 axes as symmetry axes;

(b) $\gamma = 180°$, 300° and 60° give oblate shapes;

(c) with γ not a multiple of 60°, triaxial shapes result;

(d) the interval $0° \leq \gamma \leq 60°$ is sufficient to describe all possible quadrupole deformed shapes;

(e) the increments along the three semi-axes in the body-fixed systems are evaluated as

$$\begin{aligned} \delta R_1 &= R\left(\frac{\pi}{2}, 0\right) - R_0 = R_0 \sqrt{\frac{5}{4\pi}} \beta \cos\left(\gamma - \frac{2\pi}{3}\right) \\ \delta R_2 &= R\left(\frac{\pi}{2}, \frac{\pi}{2}\right) - R_0 = R_0 \sqrt{\frac{5}{4\pi}} \beta \cos\left(\gamma + \frac{2\pi}{3}\right) \\ \delta R_3 &= R(0,0) - R_0 = R_0 \sqrt{\frac{5}{4\pi}} \beta \cos\gamma \end{aligned} \tag{12.32}$$

or, when taken together,

$$\delta R_k = R_0 \sqrt{\frac{5}{4\pi}} \beta \cos\left(\gamma - \frac{2\pi}{3}k\right) \qquad k = 1, 2, 3. \tag{12.33}$$

• In deriving the Hamiltonian describing the collective modes of motion, we start again from the collective Hamiltonian of equation (12.4) but with the potential energy changed into an expression of the type

$$U(\beta,\gamma) = \tfrac{1}{2} C_{20}(a_{20}(\beta,\gamma) - a_{20}^\circ)^2 + C_{22}(a_{22}(\beta,\gamma) - a_{22}^\circ)^2 \tag{12.34}$$

corresponding to a quadratic small amplitude oscillation but now around the equilibrium point $(a_{20}^\circ, a_{22}^\circ, a_{2-2}^\circ)$. At the same time, collective rotations can occur. Even more

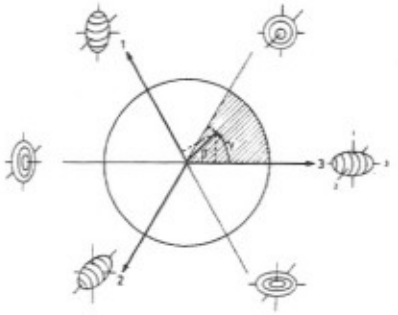

Figure 12.12. Various nuclear shapes in the (β, γ) plane. The projections on the three axes are proportional to the various increments δR_1, δR_2 and δR_3 (see equations (12.32)) (taken from Ring and Schuck 1980).

general expressions of $U(\beta, \gamma)$ can be used and, as will be pointed out in Chapter 13, microscopic shell-model calculations of $U(\beta, \gamma)$ can even be carried out. Some typical $U(\beta, \gamma)$ plots are depicted in figure 12.13 corresponding to: (i) a vibrator β^2 variation; (ii) a prolate equilibrium shape; (iii) a γ-soft vibrator nucleus and (iv) a triaxial rotor system. The more realistic example for $^{124}_{56}\mathrm{Te}_{68}$, as derived from the dynamical deformation theory (DDT), is also given in figure 12.14(a). Here, the full complexity of possible $U(\beta, \gamma)$ surfaces becomes clear: in ^{124}Te a γ-soft ridge becomes clear giving rise, after quantization, to the energy spectrum as given in figure 12.14(b). A fuller discussion on how to obtain the energy spectra after quantizing the Bohr Hamiltonian will be presented.

• The next step, the most difficult one, is the transformation of the kinetic energy term in equation (12.4). The derivation is lengthy and given in detail by Eisenberg and Greiner (1987). The resulting Bohr Hamiltonian becomes

$$H = T(\beta, \gamma) + U(\beta, \gamma) \tag{12.35}$$

with $U(\beta, \gamma)$ as given in equation (12.34) and

$$T = T_{\mathrm{rot}} + \tfrac{1}{2} B_2(\dot{\beta}^2 + \beta^2 \dot{\gamma}^2) \tag{12.36}$$

where

$$T_{\mathrm{rot}} = \frac{1}{2} \sum_{k=1}^{3} \mathcal{J}_k \omega_k^2. \tag{12.37}$$

Here, ω_k describes the angular velocity around the body-fixed axis k and $\mathcal{J}_k$ are functions of β, γ given as

$$\mathcal{J}_k = 4B_2\beta^2 \sin^2\left(\gamma - \frac{2\pi}{3}k\right) \qquad k = 1, 2, 3. \tag{12.38}$$

For fixed values of β and γ, T_{rot} is the collective rotational kinetic energy with moments of inertia $\mathcal{J}_k$. With β, γ changing, the collective rotational and β, γ vibrational energy become coupled in a complicated way. Using the irrotational value for B_2 (section 12.1), these irrotational moments of inertia become

$$\mathcal{J}_k^{\mathrm{irrot}} = \frac{3}{2\pi} m A R_0^2 \beta^2 \sin^2\left(\gamma - \frac{2\pi}{3}k\right) \qquad k = 1, 2, 3 \tag{12.39}$$

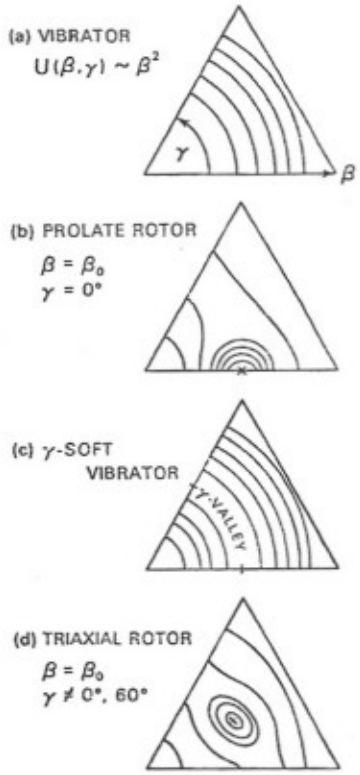

Figure 12.13. Different potential energy shapes $U(\beta, \gamma)$ in the β, $(\gamma = 0° \rightarrow \gamma = 60°)$ sector corresponding to a spherical vibrator, a prolate rotor, a γ-soft vibrator and a triaxial rotor respectively (taken from Heyde 1989).

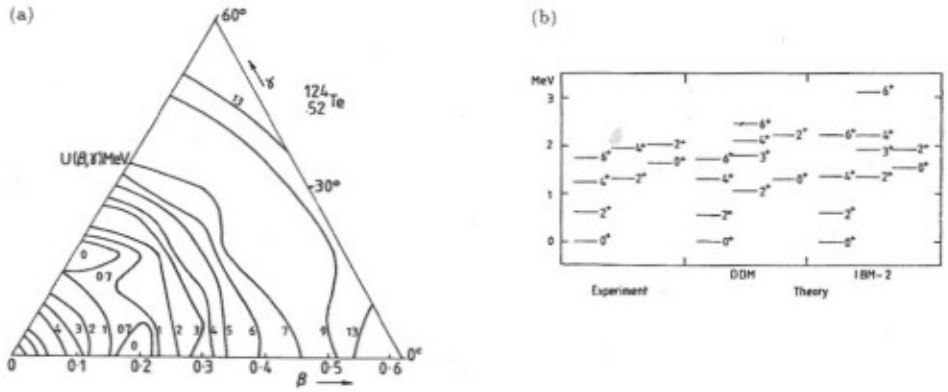

Figure 12.14. The contour plots of $U(\beta, \gamma)$ for $^{124}_{52}$Te obtained from the dynamical deformation model (DDM) calculations of Kumar (1984). The corresponding collective spectra in ^{124}Te are also given (taken from Heyde 1989).